Indian J Phys (April 2016) 90(4):469–476
DOI 10.1007/s12648-015-0776-7

ORIGINAL PAPER

Measurement of strong coupling α_s in e^+e^- annihilation using jet rate and event shape

M E Zomorrodian[1]*, M Hasheminia[2] and A Mirjalili[2]

[1]Department of Physics, Ferdowsi University of Mashhad, 91775-1436 Mashhad, Iran

[2]Physics Department, Yazd University, 89195-741 Yazd, Iran

Received: 14 June 2015 / Accepted: 20 August 2015 / Published online: 7 October 2015

Abstract: The hadronic events from the AMY data at 60 GeV center-of-mass energy are studied. We measure the coupling constant α_s first by using the three-jet rate method. From the event shape, we also extract the strong coupling constant, based on next-to-next leading order. Our results are consistent with the running of α_s expected from quantum chromodynamics predictions at next-to-next leading order corrections.

Keywords: Event shape; Jet rate; Strong coupling

PACS Nos.: 13.66.Bc

1. Introduction

Quantum chromodynamics (QCD) is generally accepted to be the correct theory for the description of strong interactions between quarks and gluons. If the quark masses and mixing angles are fixed, then the only free parameter of the theory is the strong coupling constant α_s. Many precise fits of the standard model as well as searches for new physics depend on α_s. Therefore, it is of paramount importance to measure this parameter at the best possible precision. In particular, measurements based on different underlying processes, at different energy scales, constitute an important consistency check of the theory and are used to prove the so-called running coupling constant, i.e., the decrease in the coupling strength with increasing energy scale. During the last 20 years, an enormous wealth of measurements has become available, using many different initial and final states [1–3]. Recently, theoretical progress has been made leading to a significant improvement in the prediction of the three-jet rates as a function of α_s [4]. The annihilation of an electron–positron pair into a pair of quarks provides an ideal laboratory to test the theory of the strong interaction. One method to measure the free parameter α_s is using the events with more than two jets in the final state. There are many different schemes to separate two, three, and four jets in each event. One of the most reliable of which is the JADE algorithm. In this paper, we report on the determination of the strong coupling constant from the three-jet rates, in e^+e^- annihilation using the AMY data at KEK TRISTAN. From the event shape, we also extract the strong coupling constant, at leading order (LO), next to leading order (NLO), and next-to-next leading order (NNLO). The event shape variables consist of thrust, heavy jet mass, wide jet broadening, total jet broadening, and the C-parameter. For three-jet events in electron positron annihilations, these are well-established set of infrared safe observables which are widely used [5, 6].

2. Experimental details

2.1. Detector description

The complete AMY detector, trigger, and luminosity measurements are described elsewhere [7, 8]. Here, we mention only those features which are essential for multihadron analysis. The AMY detector consists of a tracking detector and shower counter inside a 3-T solenoid magnetic coil which is surrounded by a steel flux return yoke followed by a muon detection system. The charged particle tracking detector consists of a four-layer cylindrical array

*Corresponding author, E-mail: zomorrod@um.ac.ir

of drift tubes (inner tracking chamber or ITC) and a 40-layer cylindrical drift chamber (central drift chamber or CDC) with 25 axial layers of wires and 15 stereo layers. Charged particles are detected efficiently over the polar angle region $|\cos\theta| < 0.85$ with a momentum resolution $\frac{\Delta P_t}{P_t} = 0.7\,\% \times [P_t\,(GeV/c)]$.

Radially outside of the CDC, there is a 15 radiation length cylindrical electromagnetic calorimeter (barrel shower counter or SHC) which serves as a photon detector. The detector fully covers the angular region $|\cos\theta| < 0.73$. The energy resolution is $\frac{\sigma_E}{E} \approx 23\,\%/\sqrt{E\,(GeV)} + 6\,\%$, and its angular resolution is $\sigma_\phi = 23^\circ$ and $\sigma_\theta = 0.3^\circ$. In the end-cap region, there is an electromagnetic calorimeter specialized for measuring Bhabha scattering. A schematic view of the detector is shown in Fig. 1. The description of the various detector components and the hadronic event selection criteria are given in detail in ref [7, 8].

2.2. Event selection and data correction

The data were collected with the AMY detector at the TRISTAN storage ring at KEK, Japan, in 1980. Even though the data for this analysis were recorded more than 30 years ago, the results of this study are still valuable.

Multi-hadron annihilation events were selected by requiring five or more charged tracks, a total visible energy (E_{vis}) greater than half of the center-of-mass energy, a momentum imbalance along the beam direction of magnitude $<0.4\ E_{\text{vis}}$, and more than 3 (5) GeV of energy deposited in the SHC at center-of-mass energies of (54–61.4) GeV. Monte Carlo simulations indicated those contaminations from $e^+e^- \to \tau^+\tau^-$and the two photon processes ($e^+e^- \to e^+e^- + hadrons$) were 0.9 and 1.2 %, respectively. From the way the number of selected events changed when we varied the assumed resolutions and cut criteria, we estimated the systematic error associated with the event selection procedure to be 2.3 %. The total of 16,335 hadronic events at the mean center-of-mass energy of 60 GeV satisfied the hadronic event selection criteria, the total integrated luminosity being 160 pb^{-1}.

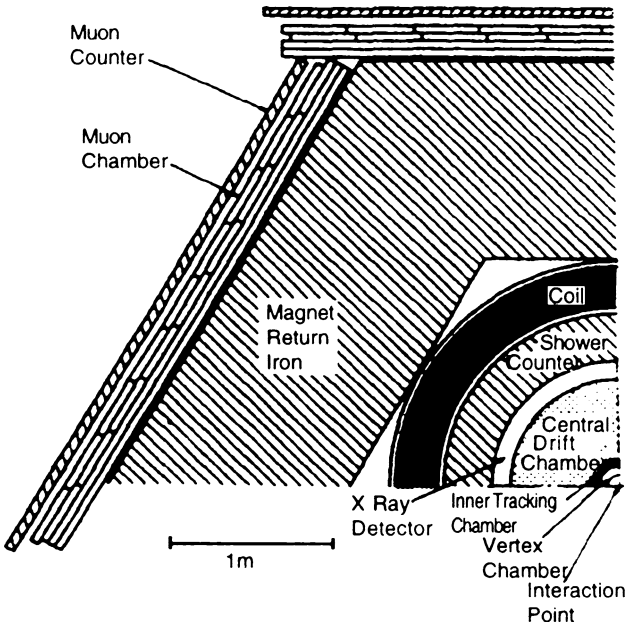

Fig. 1 AMY detector

To correct the observed distributions for detector acceptance, initial-state radiation, and the hadronic event selection criteria, events produced by Lund JETSET 6.3 or 7.3 Parton shower generators [9] were passed through programs that simulated the detector and were subjected to the same analysis procedure as was used for the actual data. Comparisons of distributions determined from the simulation with those of the generated events were used to determine bin-by-bin corrected factors. A bin-by-bin correction procedure was suitable for most quantities as the effects of finite resolution and acceptance did not cause significant migration (and therefore correlation) between bins. A number of tunable parameters were adjusted by tuning to the previously published AMY data at 60 GeV [10, 11].

The exact definition of "events from the simulation" and "generated events" which usually referred to as particle or hadron level for generator events and detector level for events after detector simulation and reconstruction was explained in detail in [7, 8, 12].

2.3. Systematic uncertainty

Several sources of systematic uncertainty were investigated. Experimental uncertainties were evaluated by repeating the analysis with different event selection cuts, reconstruction calibration versions (using different detector correction procedures and using different reconstruction softwares), samples of simulated events to derive the corrections for experimental effects, and with different fit ranges. The experimental uncertainties were dominated by the different detector calibrations and the experimental corrections based on Monte Carlo generated events. Hadronization uncertainties were estimated by changing the Monte Carlo generator for hadronization corrections from PYTHIA to HERWIG. The differences between PYTHIA and HERWIG determined this uncertainty. Theoretical systematic uncertainties were found by repeating the fits with the renormalization scale factor $x_\mu = \frac{\mu}{Q}$ being changed from $x_\mu = 1$ (AMY 60 GeV cm energy) to 0.5 or 2.

3. JADE algorithm

Jets are defined by means of JADE clustering algorithm. For each pair of i and j, the quantity y_{ij} is calculated as [13, 14]:

$$y_{ij} = \frac{2E_iE_j(1-\cos\theta_{ij})}{E_{vis}^2} \quad (1)$$

where E_i and E_j are the energies of particles i and j, θ_{ij} is the angle between the momentum directions, and $E_{\rm vis}$ is the total visible energy in the event. The pair with the smallest value of y_{ij} is found, and if this is below a given resolution parameter $y_{\rm cut}$, the pair is replaced by a pseudo-particle with four momentum $P^\mu = P_i^\mu + P_j^\mu$. The procedure is then repeated using the new set of particles and pseudo-particles. When all the values of y_{ij} are greater than $y_{\rm cut}$, the clustering procedure stops. Each particle or pseudo-particle in the event is uniquely associated with a cluster (jet).

The distribution of jet multiplicities obtained by these clustering algorithms depends on the jet resolution parameter $y_{\rm cut}$. For small $y_{\rm cut}$, many jets are found because of the hadronization of fluctuation process, whereas for large $y_{\rm cut}$, mostly two-jet events are found, and the $q\bar{q}g$ events are not resolved. However, Monte Carlo studies show that there is a range of cluster parameters, for which QCD effects can be resolved, and the fragmentation effects are sufficiently small. We have considered the fit with a range of $y_{\rm cut}$ points. We have also considered the correlations between the data points as the following [15]. The correlations between the different $y_{\rm cut}$ bins are determined using MC events. The result obtained at a center-of-mass energy of 60 GeV from the fit to the three-jet rates is shown together with the three-jet rate distribution in Fig. 2. We observe a good description of the three-jet rates by the theory. The inset of Fig. 2 shows the difference between the data and the simulation divided by the combined statistical and experimental error.

4. Results and discussion

4.1. Determination of α_s using jet rate

The fraction of multi-hadronic events in a given sample that are classified as containing n jets for a given value of the jet resolution parameter $y_{\rm cut}$ is referred to as the n jet rate. This n jet rate is explicitly defined as [16, 17]

$$R_n = \frac{\sigma_n(\mu)}{\sigma_{\rm tot}} \quad (2)$$

The arbitrary renormalization scale is denoted by μ. The production rates can be calculated within perturbation theory. The perturbative expansion of the three-jet rates reads:

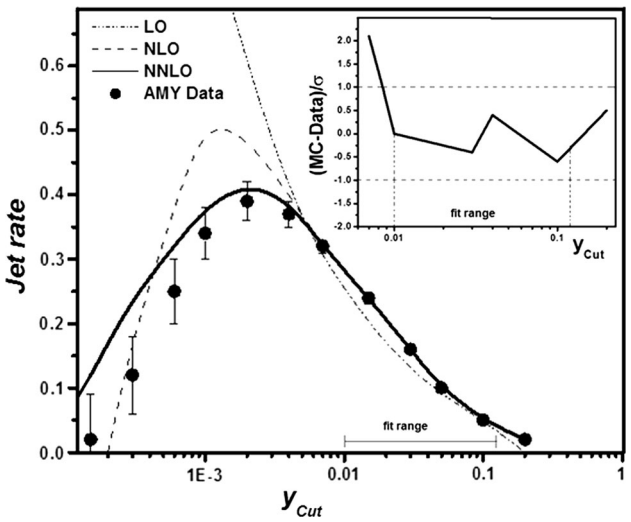

Fig. 2 Three-jet rates for different $y_{\rm cut}$s and for different QCD models for AMY data. The *inset* shows the difference between data and the simulation divided by the combined statistical and experimental error

$$R_3 = \frac{\alpha_s}{2\pi}\bar{A}_3(\mu) + \left(\frac{\alpha_s}{2\pi}\right)^2\bar{B}_3(\mu) + \left(\frac{\alpha_s}{2\pi}\right)^3\bar{C}_3(\mu) + O(\alpha_s^4) \quad (3)$$

In practice, the numerical program computes the quantities

$$\frac{\sigma_3(\mu)}{\sigma_0} = \frac{\alpha_s}{2\pi}A_3(\mu) + \left(\frac{\alpha_s}{2\pi}\right)^2 B_3(\mu) + \left(\frac{\alpha_s}{2\pi}\right)^3 C_3(\mu) + O(\alpha_s^4) \quad (4)$$

normalized to σ_0, which is the LO cross section for $e^+e^- \to hadrons$ instead of the normalization to $\sigma_{\rm tot}$. From the expansion of the total hadronic cross section $\sigma_{\rm tot}$, we have:

$$\sigma_{\rm tot}(\mu) = \sigma_0(\mu)\left(1 + \frac{\alpha_s}{2\pi}A_{\rm tot}(\mu) + \left(\frac{\alpha_s}{2\pi}\right)^2 B_{\rm tot}(\mu) + \left(\frac{\alpha_s}{2\pi}\right)^3 C_{\rm tot}(\mu) + O(\alpha_s^4)\right) \quad (5)$$

We obtain the relations between the coefficients A_3, B_3, and C_3 and the coefficients $\bar{A}_3, \bar{B}_3$ and $\bar{C}_3$:

$$\begin{aligned} \bar{A}_3 &= A_3 \\ \bar{B}_3 &= B_3 - A_{\rm tot}A_3 \\ \bar{C}_3 &= C_3 - B_{\rm tot}B_3 - (B_{\rm tot} - A_{\rm tot}^2)A_3 \end{aligned} \quad (6)$$

where

$$\begin{aligned} A_{\rm tot} &= C_F \\ B_{\rm tot} &= \frac{1}{4}\left[-\frac{3}{2}C_F^2 + C_FC_A\left(\frac{123}{2} - 44\zeta_3\right) + C_FT_RN_f(-22 + 16\zeta_3)\right] \end{aligned} \quad (7)$$

The color factors are defined as usual by

$$C_A = N, \quad C_F = \frac{N^2 - 1}{2N}, \quad T_R = \frac{1}{2} \tag{8}$$

N_c denotes the number of colors and N_f the number of light quark flavors.

It is sufficient to calculate the coefficients $\bar{A}_3, \bar{B}_3$ and $\bar{C}_3$ for a fixed renormalization scale μ^2, which can be taken conveniently to be equal to the center-of-mass energy $\mu^2 = s$ [15, 18].

Our measured three-jet cross sections are shown in Fig. 2 for our AMY data after corrections and compared with different QCD models.

By comparing our diagrams with the three QCD calculations, we observe that the agreement for each of the jet rates becomes systematically good as the order of perturbation theory increases. In other words, the distributions are more consistent with NNLO than LO or NLO corrections.

By fitting the AMY with Eq. (3), the strong coupling constant α_s is derived.

Our measurement of strong coupling constant α_s is based on χ^2 fits of QCD predictions to the corrected three-jet rate distribution. The theoretical predictions of three-jet rates using $O(\alpha_s^3)$ calculation provide distributions at the parton level. In order to confront the theory with the hadron-level data, it is necessary to correct the hadronization effects. The three-jet rates have been calculated at hadron and parton level using PYTHIA5.7 [19], HERWIG 6.2 [20], and ARIADNE 4.11 [21]. Each of these hadronization models contains a number of tunable parameters, which have been adjusted by tuning to previously published OPAL data at 91 GeV as summarized in [22] for PYTHIA and in [23] for HERWIG and ARIADNE. The theoretical prediction is then multiplied by the ratio of the hadron and parton level, (the so-called hadronization correction factor C^{had}) for three-jet rates to correct for hadronization. The fit range is determined by requiring the correction from hadronization and detector effects to be small.

The hadronization correction factors C^{had} as obtained from the three simulated generated events are shown in Fig. 3. We find that hadronization corrections have a significant dependence on y_{cut}. The difference between the models is considered as a systematic uncertainty in the fits. The fit range covers the part of the distribution at large y_{cut}, where the perturbative QCD predictions are able to adequately describe the data corrected for hadronization. The parts of the distributions at low y_{cut} are dominated by the events with more than three jets, which cannot be described accurately by the predictions. In addition, experimental and hadronization corrections become large in this region.

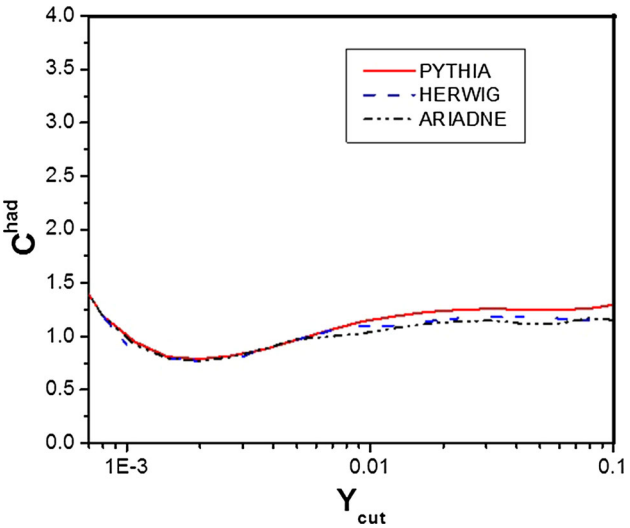

Fig. 3 Hadronization corrections for three-jet rates as calculated using PYTHIA, HERWIG and ARIADNE

The theoretical uncertainty, associated with missing higher-order terms in the theoretical prediction, has been assessed by varying the renormalization scale factor x_μ. This value is set to 0.5 and 2. The larger deviation from the default value of $x_\mu = 1$ is taken as the theoretical systematic uncertainty. By taking into accounts all correction factors, we find the value of the coupling constant up to NNLO correction as:

$$\alpha_s = 0.1257 \pm 0.0035(stat) \pm 0.0065(\text{exp}) \pm 0.0075(had) \pm 0.0041(theo)$$

with a value of the $\frac{\chi^2}{d.of} = 1.256$.

4.2. Determination of α_s using event shape distributions

The properties of hadronic events may be described by a set of event shape observables [24–26]. These may be used to characterize the distribution of particles in an event such as "pencil-like," planar, and spherical. They can be computed either using the measured charged particles and calorimeter clusters, or using the true hadrons or partons in simulated events. The following event shapes are considered here:

(a) *Thrust, T*

The global event shape variable thrust is defined as [1, 27]

$$T = \max\left(\frac{\sum \vec{p}_i.\vec{n}}{\sum |\vec{p}_i|}\right) \tag{9}$$

where $\vec{p}_i$ is the momentum vector of particle i, the thrust axis $\vec{n}$ is the unit vector which maximizes the above expression. The value of the thrust can vary between 0.5 and 1.0.

(b) *Heavy hemisphere mass M_H^2/s.*

In the original definition, one divides the event into two hemispheres. In each hemisphere, H_i, one also computes the hemisphere invariant mass as:

$$M_i^2/s = \frac{1}{E_{\rm vis}^2}\left(\left(\sum_{k\in H_I} p_k\right)^2\right) \tag{10}$$

where $E_{\rm vis}$ is the total energy visible in the event. In the original definition, the hemisphere is chosen such that $M_1^2 + M_2^2$ is minimized. We follow the more customary definition whereby the hemispheres are separated by the plane orthogonal to the thrust axis.

The larger of the two hemispheres invariant masses yields the heavy jet mass:

$$\rho \equiv M_H^2/s = \max(M_1^2/s, M_2^2/s) \tag{11}$$

(c) *Jet Broadening, B_W and B_T*

Taking a plane perpendicular to $\vec{n}_T$ through the coordinate origin, one defines two event hemispheres $H_{1,2}$. In each of them, one determines the hemisphere broadening:

$$B_i = \frac{\sum_{k\in H_i} |\vec{p}_k \times \vec{n}_T|}{2\sum_k p_k} \tag{12}$$

The wide and total jet broadening are then defined as

$$B_W = \max(B_1, B_2) \tag{13}$$

$$B_T = B_1 + B_2 \tag{14}$$

(d) *The C-parameter*

The C-parameter is derived from the eigenvalues of the linearized momentum tensor

$$\theta^{\alpha/3} = \frac{1}{\sum_k |\vec{p}_k|}\sum_k \frac{P_k^\alpha P_k^\beta}{|\vec{P}_k|}, \quad (\alpha,\beta = 1,2,3)$$

which has three eigenvalues λ_i. These eigenvalues are used to construct the C-parameter:

$$C = 3(\lambda_1\lambda_2 + \lambda_2\lambda_3 + \lambda_3\lambda_1) \tag{15}$$

The perturbative expansion for the distribution of a generic observable y up to NNLO at e^+e^- center-of-mass energy, $\sqrt{s}$, for a renormalization scale μ^2 is given by [5, 6]

$$\begin{aligned}\frac{1}{\sigma_{had}}\frac{d\sigma}{dy}(s,\mu^2,y) = &\left(\frac{\alpha_s(\mu)}{2\pi}\frac{d\bar{A}}{dy}\right) + \left(\frac{\alpha_s(\mu)}{2\pi}\right)^2 \\ &\times\left(\frac{d\bar{B}}{dy} + \frac{d\bar{A}}{dy}\beta_0\log\frac{\mu^2}{s}\right) \\ &+\left(\frac{\alpha_s(\mu)}{2\pi}\right)^3\left(\frac{d\bar{C}}{dy} + 2\frac{d\bar{B}}{dy}\beta_0\log\frac{\mu^2}{s} + \frac{d\bar{A}}{dy}\right. \\ &\left.\times\left(\beta_0^2\log^2\frac{\mu^2}{s} + \beta_1\log\frac{\mu^3 s}{s}\right)\right) + O(\alpha_S^4)\end{aligned} \tag{16}$$

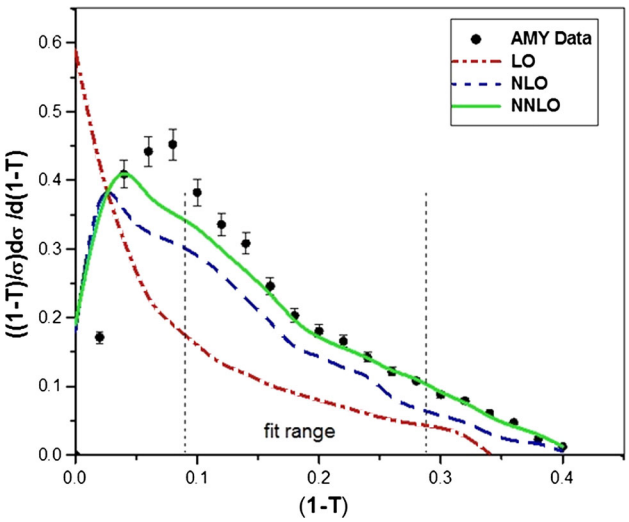

Fig. 4 Thrust distribution at LO (*dashed dotted*), NLO (*dashed*), and NNLO (*solid*) with $\alpha_s = 0.1241$ compared to experimental data from AMY

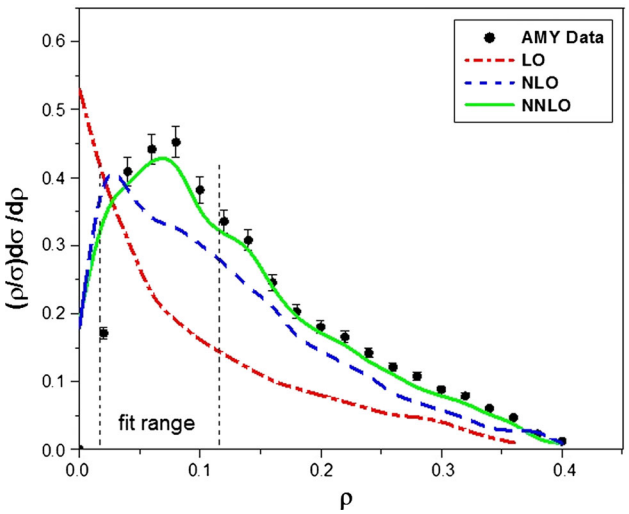

Fig. 5 Heavy jet mass distribution at LO (*dashed dotted*), NLO (*dashed*), and NNLO (*solid*) with $\alpha_s = 0.1213$ compared to experimental data from AMY

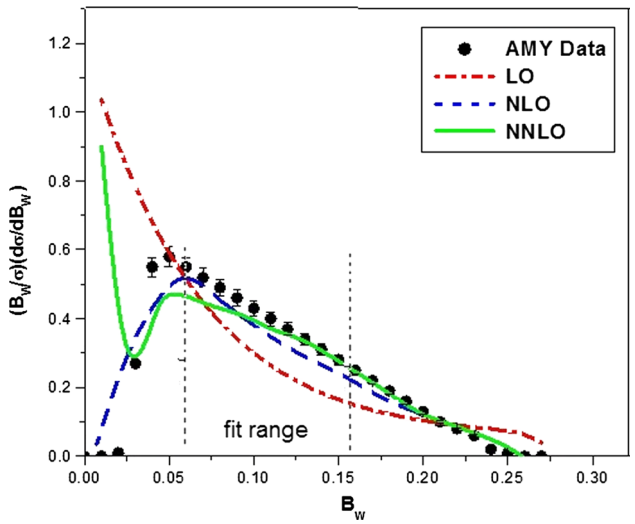

Fig. 6 Wide jet broadening distribution at LO (*dashed dotted*), NLO (*dashed*), and NNLO (*solid*) with $\alpha_s = 0.1209$ compared to experimental data from AMY

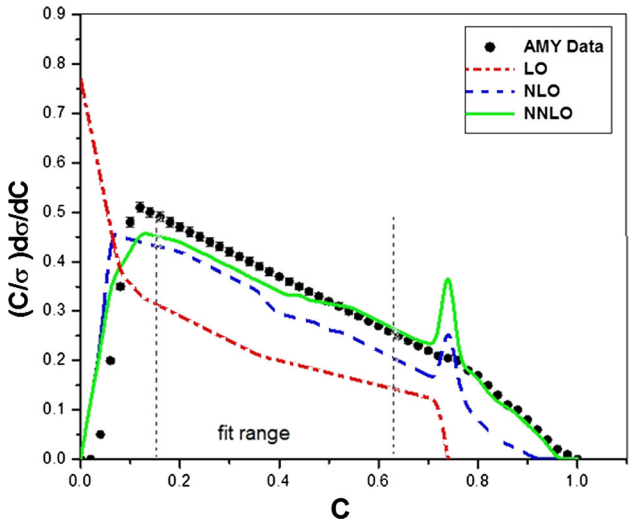

Fig. 8 C-parameter distribution at LO (*dashed dotted*), NLO (*dashed*), and NNLO (*solid*) with $\alpha_s = 0.1214$ compared to experimental data from AMY

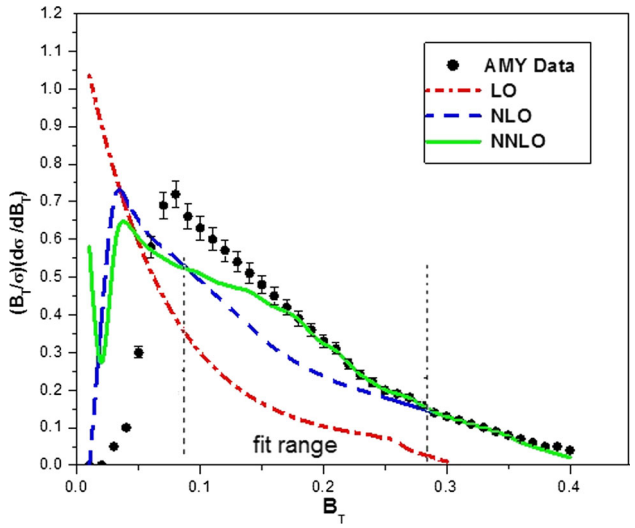

Fig. 7 Total jet broadening distribution at LO (*dashed dotted*), NLO (*dashed*), and NNLO (*solid*) with $\alpha_s = 0.1250$ compared to experimental data from AMY

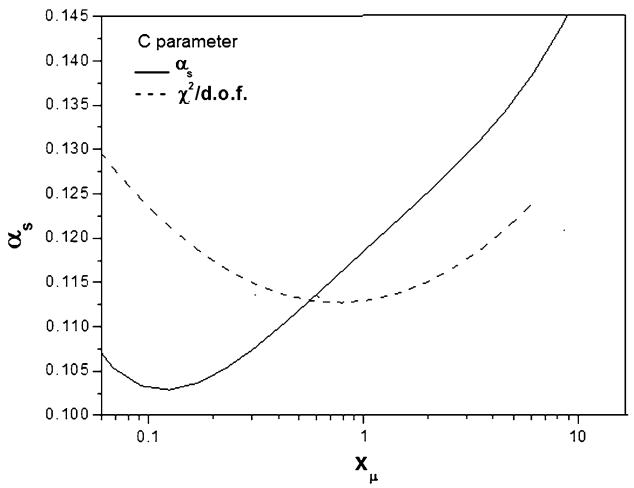

Fig. 9 Residual dependence of the fitted value of α_s and uncertainty χ^2 on the renormalization scale

where

$$\beta_0 = \frac{11C_A - 4T_R N_F}{6} \tag{17}$$

$$\beta_1 = \frac{17C_A^2 - 10C_A T_R N_F - 6C_F T_R N_F}{6}, \tag{18}$$

where the QCD color factors are

$$C_A = N, \quad C_F = \frac{N^2 - 1}{2N}, \quad T_R = \frac{1}{2} \tag{8}$$

For $N = 3$ colors and N_F light quark flavors. $\bar{A}$ gives the LO result, $\bar{B}$ is the NLO correction, and $\bar{C}$ is the NNLO correction. These coefficients have been computed for several event shape variables [5, 6]. Our calculation is carried out using a newly developed parton-level event generator program EERAD3 [15].

The measured normalized differential cross sections for each of the five event shapes after correction are shown in Figs. 4–8. As the figures indicate, the distributions for AMY are more consistent with NNLO compared to NLO or LO calculations. We expect more consistency between our data and the theory, if we take into account the higher-order QCD calculations.

At this stage, we explain the fitting procedure to find α_s. The interval of each event shape parameter used to determine α_s has been restricted to a region where non-perturbative hadronization effects are expected to be small. This

Table 1 α_s values for AMY data for different event shapes and their relative x_μ that uncertainty becomes minimized

Variable	α_s	Statistical	Experimental	Hadronization	Theoretical	x_μ	$\chi^2/d.o.f$	Fit range
1-T	0.1241	±0.0041	±0.0065	±0.0074	±0.0043	0.84	1.01	0.09–0.28
ρ	0.1213	±0.0035	±0.0065	±0.0071	±0.0035	0.91	1.17	0.02–0.12
B_T	0.1250	±0.0044	±0.0065	±0.0081	±0.0029	0.85	1.23	0.08–0.28
B_W	0.1209	±0.0041	±0.0065	±0.0078	±0.0030	0.76	1.11	0.06–0.16
C	0.1214	±0.0052	±0.0065	±0.0070	±0.0045	0.95	1.04	0.15–0.65

Table 2 Results $R = \frac{y}{\sigma}\frac{d\sigma}{dy}$ at $\sqrt{s} = 60\ GeV$ (*AMY*) for the event shape observables y. (First error is statistical, the second systematic)

y=1-T	R(y)
0-0.03	0.40865±0.0035±0.0058
0.03-0.06	0.44171±0.0041±0.0064
0.06-0.09	0.38161±0.0042±0.0063
0.09-0.12	0.33534±0.0037±0.0058
0.12-0.15	0.24596±0.0043±0.0059
0.15-0.18	0.20308±0.0037±0.0056
0.18-0.21	0.16577±0.0041±0.0064
0.21-0.24	0.14212±0.0041±0.0064
0.24-0.27	0.10779±0.0041±0.0064
0.27-0.3	0.08813±0.0041±0.0064
0.30-0.33	0.06065±0.0041±0.0064
0.33-0.36	0.04709±0.0041±0.0064
0.36-0.39	0.01202±0.0041±0.0064

y= B_T	R(y)
0-0.03	0
0.03-0.06	0.30±0.0026±0.0051
0.06-0.09	0.72±0.0027±0.0056
0.09-0.12	0.6±0.0029±0.0059
0.12-0.15	0.51±0.0031±0.0055
0.15-0.18	0.42±0.0028±0.0048
0.18-0.21	0.33±0.0031±0.0053
0.21-0.24	0.24±0.0039±0.0061
0.24-0.27	0.19±0.0036±0.0052
0.27-0.30	0.14±0.0035±0.0053
0.30-0.33	0.11±0.0038±0.0061
0.33-0.36	0.08±0.0038±0.0057
0.36-0.39	0.05±0.0034±0.0055

y=C	R(y)
0-0.07	0.2±0.0029±0.0048
0.07-0.14	0.51±0.0034±0.0051
0.08-0.1	0.48±0.0037±0.0059
0.14-0.21	0.47±0.0041±0.0064
0.21-0.28	0.44±0.0042±0.0058
0.28-0.35	0.4±0.0035±0.0057
0.35-0.42	0.37±0.0031±0.0059
0.42-0.49	0.34±0.0029±0.0061
0.49-0.56	0.3±0.0031±0.0049
0.56-0.63	0.26±0.0041±0.0054
0.63-0.70	0.24±0.0035±0.0058
0.70-0.80	0.06±0.0039±0.0062
0.80-1	0.08±0.0031±0.0061

y= B_W	R(y)
0-0.02	0
0.02-0.04	0.55±0.0037±0.0059
0.04-0.06	0.58±0.0033±0.0057
0.06-0.08	0.52±0.0031±0.0056
0.08-0.1	0.46±0.0039±0.0052
0.1-0.12	0.4±0.0037±0.0061
0.12-0.14	0.34±0.0032±0.0055
0.14-0.16	0.28±0.0038±0.0054
0.16-0.18	0.22±0.0036±0.0062
0.18-0.2	0.16±0.0034±0.0063
0.2-0.22	0.1±0.0031±0.0049
0.22-0.24	0.06±0.0037±0.0052
0.24-0.26	0.01±0.0029±0.0048

y= ρ	R(y)
0-0.03	0.17±0.0041±0.0063
0.03-0.06	0.44±0.0039±0.0059
0.06-0.09	0.45±0.0040±0.0061
0.09-0.12	0.33±0.0037±0.0058
0.12-0.15	0.31±0.0039±0.0065
0.15-0.18	0.20±0.0035±0.0056
0.18-0.21	0.18±0.0032±0.0059
0.21-0.24	0.14±0.0028±0.0049
0.24-0.27	0.11±0.0032±0.0056
0.27-0.3	0.09±0.0027±0.0047
0.3-0.33	0.06±0.0026±0.0045
0.33-0.36	0.05±0.0032±0.0049
0.36-0.39	0.01±0.0039±0.0057

has been determined by examining the hadron and parton level for the event shape distribution from a number of patron shower-based Monte Carlo models: PYTHIA 5.7, HERWIG 6.2, and ARIADNE 4.11. As mentioned above, the parameters of these models have been tuned using data from OPAL experiment at the 91 GeV center-of-mass energy.

The uncertainty due to the choice of the renormalization scale $x_\mu = {}^{\mu}/_{\sqrt{s}}$ yields a large contribution to the total error. Consequently, missing higher orders, whose effects on the values of the coupling are assessed by varying, x_μ, are still important. The fitted values for α_s change considerably for different choices of the scale. This is demonstrated in Fig. 9 for the C-parameter in 60 GeV center-of-mass energy. The plot shows the strong dependence of the fitted α_s on the renormalization scale factor x_μ. The real value of α_s has been estimated by comparing theory with data using the minimum of χ^2 in this figure, such that everywhere χ^2 is minimum, its corresponding α_s becomes our real strong coupling constant. Separate fits have been performed to each of the five observables at 60 GeV center-of-mass energy, indicating x_μ as a free parameter. Table 1 lists the values of α_s extracted by this method for different observables together with their relative x_μ which makes the uncertainty become minimized, as well as the $\frac{\chi^2}{d.o.f}$ and fit range separately for each parameter. The thrust as well as the C distributions are well described by the QCD analysis giving us a better fit with a lower χ^2. With the other three observables, B_T, B_W, and ρ, we also find generally consistent results with standard QCD and previous measurements [28–31] but with a larger χ^2. Our interpretation is that the QCD calculations for $1 - T$ and C provide a better description of the data compared to B_T, B_W, and ρ. We conclude that all five observables give us a reasonable and a satisfactory result within the statistical uncertainty. The numerical values for all the event shape distributions are listed in Table 2.

5. Conclusions

We have presented in this paper measurements of the coupling constant α_s for hadronic events produced at AMY at 60 GeV center-of-mass energy. Experimental uncertainties have been evaluated by repeating the analysis with different event selection cuts, reconstruction calibration versions, samples of simulated events to derive the corrections for experimental effects and with different fit ranges. The experimental uncertainties are dominated by the different detector calibrations and the experimental corrections based on Monte Carlo generated events. Hadronization uncertainties have been estimated by changing the Monte Carlo generator for hadronization corrections from PYTHIA to HERWIG. The differences between PYTHIA and HERWIG determine this uncertainty. Theoretical systematic uncertainties have been found by repeating the fits with the renormalization scale factor $x_\mu = \frac{\mu}{Q}$ changed from $x_\mu = 1$(AMY 60 GeV cm energy) to 0.5 or 2. The precise determination of α_s is obtained by using both three-jet rates and event shape distributions at LO, NLO and NNLO. In general, the NNLO provides the best description. The result extracted from the event shape is also consistent with the running of α_s expected from the QCD predictions.

Acknowledgments We would like to acknowledge the KEK staff and the AMY collaboration for giving us the opportunity of using the AMY data for this analysis.

References

[1] O Biebel *Phys. Rep.* **340** 165 (2001)
[2] E Heister *Eur. Phys. J.* **C35** 457 (2004)
[3] T Ghaffary, A Sepehri, M Hasheminia and M E Zomorrodian *Indian. J. Phys*. **83** 1691 (2009)
[4] J Schick, S Bethke, O Biebel and S Kluth *Eur. Phys. J.* **C48** 3 (2006)
[5] S Weinzierl, *JHEP **0906*** 041 (2009)
[6] S Weinzierl, *Phys. Rev*. **D80** 094018 (2009)
[7] T Kumita et al., *Phys. Rev*. **D42** 1339 (1990)
[8] Y K Li et al., *Phys. Rev*. **D9** 2675 (1990)
[9] T Sjostrand and M Bengtsson *Comput. Phys. Commun*. **43** 367 (1987)
[10] T Mori et al., *Phys. Lett*. **B218** 499 (1989)
[11] T Mori et al., PhD Thesis (University of Rochester) (1988)
[12] S Eno et al., *Phys. Rev. Lett*. **63** 1910 (1989)
[13] O Adriani et al., *Phys. Rep*. **236** 1 (1993)
[14] W Bartel et al., *Z. Phys.* **C33** 23 (1986)
[15] J Schieck et al., *Nucl. Phys. Proc. Suppl.* **234** 225 (2013)
[16] A Gehrmann et al., *Comput. Phys. Commun*. **185** 3331 (2014)
[17] A Gehrmann et al., *Phys. Rev. Lett*. **100** 172001 (2008)
[18] S Weinzierl *Eur. Phys. J.* ***C*71** 1565 (2011)
[19] T Sjöstrand, *Comp. Phys. Comm*. **82** 74 (1994)
[20] G Marchesini et al., *Comp. Phys. Comm*. **67** 465 (1992)
[21] L Lönnblad, *Comp. Phys. Comm***. 71** 15 (1992)
[22] G. Alexander et al., *Zeit. Phys.* **C69** 543 (1996)
[23] G. Abbiendi et al., *Eur. Phys. J.* **C35** 293 (2004)
[24] G Dissertori et al., *Nuovo Cim*. ***C*033N2** 67 (2010)
[25] M Dasgupta and G P Salam *J. Phys*. **G30** R143(2004)
[26] P Achard et al., *Phys. Lett.* ***B*536** 217 (2002)
[27] G Dissertori et al., *JHEP* **080** 2040 (2008)
[28] S Kluth *arXiv: hep-ex/1206.0065* (2012)
[29] S Bethke *26th Int. Conf. on HENP* (Dallas) (1992)
[30] S Mart'l I Garc'la *Conference C97-04-14, arXiv: hep-ex/9704016v2* (1997)
[31] S Bethke et al., *Eur. Phys. J.* ***C*64** 689 (2009)